Arch. Mech., **52**, 4–5, pp. 685–711, Warszawa 2000

Iterative methods for solution of contact optimization problems

Dedicated to Professor Zenon Mróz
on the occasion of his 70^{th} birthday

I. PÁCZELT

University of Miskolc, Miskolc, Hungary

NUMERICAL TREATMENT of frictionless contact optimization problems is presented on the basis of linear elasticity. The minimum of the pressure maximum or other mechanical values (torque, frictional power loss) is sought by controlling the pressure distribution. Smooth contact pressure distribution can be achieved by using an appropriate controlling function on the controlling subdomain. The contact problems are investigated by means of the principle of minimum complementary energy and using the augmented Lagrangian technique. Axially symmetric problems are discretized by p-version finite elements. The optimal shape of a roller bearing is determined by the application of a new controlling function, which takes the rigid body translation and rotation of the roller into consideration. Effectiveness of the proposed algorithms is demonstrated by numerical examples.

1. Introduction

IN ENGINEERING PRACTICE, connections of machine elements are frequently modeled as unilateral contact problems. The contact surfaces should be shaped in such a way that the arising contact stresses remain under a prescribed limit. Consequently, the singularity in the stress field and the danger of fatigue can be eliminated, further only low level wearing can take place on the contacting surfaces.

Contact optimization problems can be divided into two groups. The first group of problems is based on kinematical quantities [1], while the second group of the problems is using dynamical parameters.

In the first case, the following kinematical quantities are minimized in a certain region of one of the bodies (or in several regions of both bodies): the absolute value of the displacement vector, the difference between the largest and the smallest displacement projected on a given direction etc. Let us suppose that the theory of linear elasticity is applicable, and friction is not taking place between the bodies.

The kinematical optimization problem is solved in two steps.

Step 1. We solve the mathematical programming problem, which is linear or quadratic, depending on the objective function. The solution involves the contact pressure.

Step 2. Knowing the contact pressure and using the geometrical condition between the bodies, we determine the shape of that body for which the objective function is not composed [1].

In the second case, when dynamical quantities are minimized during the optimization, we can set up the following problems:

Problem 1. Minimization of the contact pressure maximum.

Problem 2. Optimization of the contact pressure taking also the frictional power loss into account.

Problem 3. Optimization problem for minimization of the maximum equivalent stress.

Problem 4. Maximization of any mechanical value (torque, force...).

The papers by CONRY [2], KLARBRING [3] and PETERSON [4] are concerned with constant contact pressure distribution. The mathematical background is given for these problems by HASLINGER and NEITTAANMAKI [5]. Numerical solutions are given by KLARBRING [3] and ODA *et al.* [6] for contact problems of an elastic or elastic-plastic punch and a rigid target, using displacement based linear and quadratic finite elements. Approximately constant contact pressure distribution is achieved in [6] and [7] by appropriate shape optimization for axially-symmetric bodies assuming that a change in radius has no effect on the stiffness and compliance matrices. A number of papers e.g. OH *et al.* [8], HARNETT [9], CHIU *et al.* [10], de MUL *et al.* [11], PÁCZELT *et al.* [12] are devoted to the issue of the roller's rounding-off. In these papers except the last one the radius of the rounding-off is given, which results in generally non-smooth contact pressure distribution. Works [13, 14] and [12] give solutions for 2D and 3D problems, provided that the contact pressure distribution is influenced by partial controlling of the contact pressure and by minimizing the maximum of the contact pressure.

Discretization of the domain with p-version finite elements is advantageous (SZABÓ *et al.* [15]), since it results in fast convergence, and the high order mapping assures accurate geometry for the shape optimization.

In this paper axially symmetric and 3D contact shape optimization problems, have been investigated. In case of axially symmetric problems the contact pressure is controlled on the whole contact region, and the p-extension of the finite element method is applied for the discretization. For 3D problems, the contact pressure is controlled only partially on the contact surface and the punch performs a rigid body rotation in addition to the rigid body translation.

2. Formulation of the contact problem

Let us consider the contact problem of two elastic bodies ($e = 1, 2$). The surfaces of the bodies will be divided into three regions: S_u^e denotes that part of the body where displacements $\mathbf{u}_o$ are given, in S_t^e the traction $\mathbf{t}_o$ is applied, while S_c^e represents that part of the bodies where contact is expected. The S_c^e part of the body is called the proposed zone of the contact. The bodies are loaded by the body force $\mathbf{b}^e$, initial stress $\mathbf{T}_o^e$ and initial strain $\mathbf{A}_o^e$. We are interested in finding the displacement vector field $\mathbf{u}$, strain $\mathbf{A}$ and stress $\mathbf{T}$ tensor fields. In the domain V^e we have the equilibrium equation

$$\mathbf{T}^e \cdot \nabla + \mathbf{b}^e = \mathbf{0}, \qquad \mathbf{r} \in V^e, \tag{2.1}$$

the strain-displacement relationship

$$\mathbf{A}^e = \frac{1}{2}\left(\mathbf{u}^e \circ \nabla + \nabla \circ \mathbf{u}^e\right), \qquad \mathbf{r} \in V^e, \tag{2.2}$$

and Hooke's constitutive law:

$$\mathbf{T}^e = \mathbf{T}_o^e + \mathbf{D}^e \cdot\cdot \left(\mathbf{A}^e - \mathbf{A}_o^e\right), \qquad \mathbf{r} \in V^e, \tag{2.3}$$

where $\mathbf{D}^e$ is a fourth-order tensor of the material parameters, "$\cdot$", "$\cdot\cdot$", "$\circ$", is the symbol of a scalar, double scalar and tensor product, respectively, and ∇ is the Hamiltonian differential operator.

The boundary conditions are:

$$\mathbf{u}^e = \mathbf{u}_o, \qquad \mathbf{r} \in S_u^e, \tag{2.4}$$

and

$$\mathbf{T}^e \cdot \mathbf{n}^e = \mathbf{t}_o, \qquad \mathbf{r} \in S_t^e. \tag{2.5}$$

For the examination of the contact/separation conditions in the proposed zone of contact, we shall consider the projection of the displacement in a prescribed direction only (e.g., normal to the surface $\mathbf{n}_c$). The contact normal vector $\mathbf{n}_c$ determines the points Q_1, Q_2 on the corresponding surfaces S_c^1 and S_c^2, where the two surfaces may contact each other (see Fig. 1). Therefore the contact surface will be denoted by S_c. We denote the displacement projected in the direction of $\mathbf{n}_c$ by $u_N^e = \mathbf{u}^e \cdot \mathbf{n}_c$, the normal stress by $\sigma_N^e = \mathbf{n}^e \cdot \mathbf{T}^e \cdot \mathbf{n}^e$ and the initial gap between bodies by h. We define the distance (gap) after deformation

$$d = d(\mathbf{u}) = u_N^2 - u_N^1 + h \geq 0, \tag{2.6}$$

and the contact pressure

$$p = -\mathbf{n}^1 \cdot \mathbf{T}^1 \cdot \mathbf{n}_c = \mathbf{n}^2 \cdot \mathbf{T}^2 \cdot \mathbf{n}_c \cong -\mathbf{n}^1 \cdot \mathbf{T}^1 \cdot \mathbf{n}^1 = -\mathbf{n}^2 \cdot \mathbf{T}^2 \cdot \mathbf{n}^2 \geq 0. \tag{2.7}$$

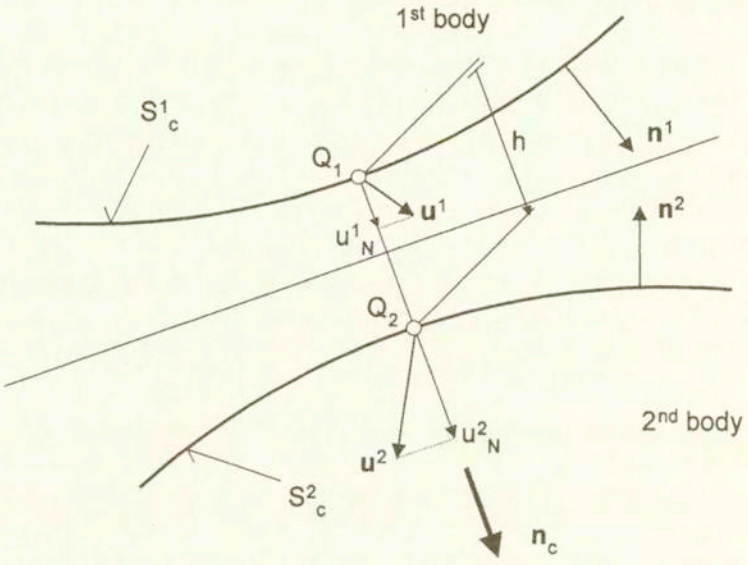

FIG. 1. Normal displacements u_N^e $(e = 1, 2)$.

Denoting the contact zone by C and the separation (gap) zone by G $(S_c = C \cup G)$, we have

$$d = 0, \qquad p \geq 0, \qquad \mathbf{r} \in C, \tag{2.8}$$

$$d > 0, \qquad p = 0, \qquad \mathbf{r} \in G, \tag{2.9}$$

$$pd = 0, \qquad \mathbf{r} \in S_c. \tag{2.10}$$

From the condition of frictionless contact we have zero tangential stress

$$\tau^e = \mathbf{e}_\tau^e \cdot \mathbf{T}^e \cdot \mathbf{n}^e = 0, \qquad \mathbf{r} \in S_c^e, \tag{2.11}$$

where $\mathbf{e}_\tau^e$ is a tangential unit vector.

If one of the bodies – let us suppose it to be the first one – can move as a rigid body, the equilibrium equations for this body must be satisfied

$$\mathbf{F} = \mathbf{F}_o - \int_{S_c^1} p\mathbf{n}_c dS = \mathbf{0}, \qquad \mathbf{M} = \mathbf{M}_o - \int_{S_c^1} \mathbf{r} \times \mathbf{n}_c p dS = \mathbf{0}, \tag{2.12}$$

where $\mathbf{F}_o, \mathbf{M}_o$ are the resultant force and moment at the origin of the coordinate system, and $\mathbf{r}$ is the position vector, "$\times$" is the symbol of a vector product.

3. Weak formulation

3.1. Principles based on the total potential energy

For investigation of the normal contact problem we can use the principle of minimum potential energy $\Pi(\mathbf{u})$ subject to two types of kinematic conditions: $\mathbf{u} = \mathbf{u}_o$ on $\mathbf{r} \in S_u$ and $d \geq 0$ on $\mathbf{r} \in S_c$.

Formally

$$\min\{\Pi(\mathbf{u}) \mid \quad \mathbf{u} = \mathbf{u}_o, \quad \mathbf{r} \in S_u, \quad d \geq 0, \quad \mathbf{r} \in S_c\}, \tag{3.1}$$

which must be solved satisfying the variational inequality $\delta\Pi \geq 0$. The detailed mathematical discussion of this variational inequality and other variational principles can be found in books by HASLINGER *et al.* [5], KIKUCHI *et al.* [16] and in the paper by TELEGA [17].

Here

$$\Pi(\mathbf{u}) = \sum_{e=1}^{2} \left\{ \frac{1}{2} \int_{V^e} (\mathbf{A}(\mathbf{u}) - \mathbf{A}_o) \cdot\cdot \mathbf{D} \cdot\cdot (\mathbf{A}(\mathbf{u}) - \mathbf{A}_o)\, dV \right. \tag{3.2}$$

$$\left. + \int_{V^e} \mathbf{A}(\mathbf{u}) \cdot\cdot \mathbf{T}_o\, dV - \int_{V^e} \mathbf{u} \cdot \mathbf{b}\, dV - \int_{S_t^e} \mathbf{u} \cdot \mathbf{t}_o\, dS \right\}.$$

Practically, instead of the problem (3.1) we can use another method, in which the contact constraints can be introduced via the Lagrangian multipliers or penalty terms. In the Lagrangian multiplier technique we are taking the variation of the following functional

$$\mathcal{L}^{LA} = \mathcal{L}^{LA}(\mathbf{u}, p) = \Pi(\mathbf{u}) - \int_{S_c} p d(\mathbf{u})\, dS \tag{3.3}$$

with respect to $\mathbf{u}$ and p satisfying the conditions $\mathbf{u} = \mathbf{u}_o \quad \mathbf{r} \in S_u, \quad p \geq 0 \quad \mathbf{r} \in S_c$ respectively, that is

$$\delta_u \mathcal{L}^{LA} = 0, \qquad -\delta_p \mathcal{L}^{LA} \geq 0. \tag{3.4}$$

In the penalty method we have the next functional

$$\mathcal{L}^{PE} = \mathcal{L}^{PE}(\mathbf{u}) = \Pi(\mathbf{u}) + \frac{1}{2} \int_{S_c} c_N \left(d^-(\mathbf{u})\right)^2 dS, \tag{3.5}$$

where $c_N >> 0$ is the penalty parameter, and d^- denotes the negative part of d. From the variational equation $\delta_u \mathcal{L}^{PE} = 0$ we have a formula for contact pressure

$$p = -c_N d^- (\mathbf{u}) . \tag{3.6}$$

As $c_N \to \infty$ we have $d^- (\mathbf{u}) \to 0$, that is the $d \geq 0$ condition can be satisfied approximately. The correct choice of the penalty parameter is essential, because the condition number of the coefficient matrix increases as the penalty parameter increases. Using p-version finite elements [15, 18], $c_N \sim 100E - 1000E$ is recommended, where E is the Young modulus.

Combining the Lagrangian method and penalty method we have the augmented Lagrangian functional in the form:

$$\mathcal{L}^{AU} = \mathcal{L}^{AU} (\mathbf{u}) = \Pi (\mathbf{u}) - \int_C p d (\mathbf{u}) \, dS + \frac{1}{2} \int_C c_N (d (\mathbf{u}))^2 \, dS, \tag{3.7}$$

where p is the Lagrangian multiplier, which is kept constant during an iteration loop. From the variational equation $\delta_u \mathcal{L}^{AU} = 0$ we have a formula for the normal contact stress

$$\sigma_N^1 = \sigma_N^2 = - (p - c_N d (\mathbf{u})) . \tag{3.8}$$

During the iteration process, the contact pressure is updated using the formula:

$$p^{(k)} = \left\langle p^{(k-1)} - c_N d \left(\mathbf{u}^{(k)} \right) \right\rangle , \tag{3.9}$$

where the operation $< \cdot >$ is defined by

$$\langle p \rangle = \frac{1}{2} (p + |p|) . \tag{3.10}$$

In the $(k+1)th$ iteration loop the contact surface is subjected to $p^{(k)}$ as an external load in the variational formula:

$$\delta_u \mathcal{L}^{AU} \left(\mathbf{u}^{(k+1)} \right) = \delta \Pi \left(\mathbf{u}^{(k+1)} \right) - \int_C \delta d (\mathbf{u}) \left(p^{(k)} - c_N d \left(\mathbf{u}^{(k+1)} \right) \right) dS = 0. \tag{3.11}$$

3.2. Principle based on the modified complementary energy

Introducing the Green's function $H^e (\mathbf{x}, \mathbf{x}')$ and the normal displacement $u^e_{N,\text{load}}$ due to the given loads, the rigid body displacement of the punch (body 1) projected in normal direction is

$$u_R (\mathbf{x}) = [\lambda_F + \lambda_M \times \mathbf{r} (\mathbf{x})] \cdot \mathbf{n}_c (\mathbf{x}) , \tag{3.12}$$

where $\lambda_F = [\lambda_{F1} \quad \lambda_{F2} \quad \lambda_{F3}]$ is the rigid body translation vector, $\lambda_M = [\lambda_{M1} \quad \lambda_{M2} \quad \lambda_{M3}]$ is the rigid body rotation vector. Then we have the following functional to be minimized:

$$\mathcal{L}^C = \mathcal{L}^C(\mathbf{p}, \lambda_F, \lambda_M) = \frac{1}{2} \int_{S_c} \int_{S_c'} p(\mathbf{x}) \left(H^1(\mathbf{x}, \mathbf{x}') + H^2(\mathbf{x}, \mathbf{x}')\right) p(\mathbf{x}')\, dS' dS + \int_{S_c} p\left(u^2_{N,\text{load}} - u^1_{N,\text{load}} + h\right) dS - \lambda_F \cdot \mathbf{F} - \lambda_M \cdot \mathbf{M}. \tag{3.13}$$

The following variational equations and inequalities can be written:

$$\delta_{\lambda_F, \lambda_M} \mathcal{L}^C = 0, \tag{3.14}$$

which give the equilibrium equations for the punch (body 1) performing rigid-body displacement, and

$$\delta_p \mathcal{L}^C \geq 0, \qquad p \geq 0 \qquad \mathbf{x} \in S_c \tag{3.15}$$

represent here the contact and separation conditions (2.8) – (2.10).

4. Discretization of the functional

4.1. Approximation of the displacement and contact pressure fields

The displacements of the contacting bodies are approximated in the usual form

$$\mathbf{u}^e = \mathbf{u}^e(\mathbf{x}) = \mathbf{N}^e(\mathbf{x})\, \mathbf{q}^e, \tag{4.1}$$

where the shape functions consist of nodal points modes, side modes and internal modes, and $\mathbf{q}^e$ is the vector of displacement parameters [15]. The p-version computation is based on this approximation resulting in high degree of accuracy. The strain vector is given by the following formula:

$$\mathbf{A}^e \to \varepsilon^e = \varepsilon(\mathbf{x}) = \partial \mathbf{u}^e = \mathbf{B}^e(\mathbf{x})\, \mathbf{q}^e, \tag{4.2}$$

where $\mathbf{B}^e(\mathbf{x})$ is the strain-displacement matrix. The stress vector can be expressed as

$$\mathbf{T}^e \to \sigma^e = \sigma^e(\mathbf{x}) = \sigma^e_o(\mathbf{x}) + \mathbf{D}^e(\mathbf{x}) \left(\mathbf{B}^e(\mathbf{x})\, \mathbf{q}^e - \varepsilon^e_o(\mathbf{x})\right), \tag{4.3}$$

where $\mathbf{D}^e(\mathbf{x})$ is the constitutive matrix, $\varepsilon_o^e, \sigma_o^e$ are the initial strain and stress vectors, respectively. Using (4.1) – (4.3), the total potential energy (3.2) can be written in discretized form:

$$\Pi^e(\mathbf{u}) \to \Pi^e(\mathbf{q}^e) = \frac{1}{2}\mathbf{q}^{eT}(\mathbf{K}^e\mathbf{q}^e - 2\mathbf{f}^e), \tag{4.4}$$

where

$$\mathbf{K}^e = \int_{V_e} \mathbf{B}^{eT}\mathbf{D}^e\mathbf{B}^e dV \tag{4.5}$$

is the element stiffness matrix,

$$\mathbf{f}^e = \int_{V_e} \mathbf{N}^{eT}\mathbf{b}^e dV + \int_{S_t^e} \mathbf{N}^{eT}\mathbf{t}_o\, dS + \int_{V^e} \mathbf{B}^{eT}(\mathbf{D}^e\varepsilon_o^e - \sigma_o^e)\, dV \tag{4.6}$$

is the element load vector, and T denotes the transpose of a matrix.

The approximation of the contact pressure by a function of class C^o is recommended

$$p = p(\mathbf{x}) = \mathbf{P}^T(\mathbf{x})\,\mathbf{p} = [P_1 \quad P_2 \quad \ldots]\,\mathbf{p}, \qquad \mathbf{x} \in S_c, \tag{4.7}$$

where $\mathbf{p}$ is the column matrix of contact pressure at the nodes, P_i is the coordinate function of the *i-th* node.

The gap occuring after deformation is computed by the following projection:

$$d = u_N^2 - u_N^1 + h = -\mathbf{L}^1(\mathbf{x})\mathbf{q}^1 + \mathbf{L}^2(\mathbf{x})\mathbf{q}^2 + h = \mathbf{L}(\mathbf{x})\mathbf{q} + h, \tag{4.8}$$

where the matrix of shape functions $\mathbf{L}^e(\mathbf{x})$ is constructed by the use of $\mathbf{N}^e(\mathbf{x})$ and the definition of the normal displacement u_N^e. The vector of displacement parameters for the whole system is given as $\mathbf{q}^T = [\mathbf{q}^{1T} \quad \mathbf{q}^{2T}]$.

The last integral in the functional (3.3) can be approximated in the following way:

$$\int_{S_c} pd\, dS = \mathbf{p}^T \int_{S_c} \mathbf{PL}\, dS\, \mathbf{q} + \mathbf{p}^T \int_{S_c} \mathbf{P}h\, dS = -\mathbf{p}^T([\mathbf{G}^1\ \mathbf{G}^2]\,\mathbf{q} - \mathbf{h}) \tag{4.9}$$

$$= -\mathbf{p}^T\mathbf{G}\mathbf{q} + \mathbf{p}^T\mathbf{h} = \mathbf{p}^T\mathbf{d},$$

where $\mathbf{d} = -\mathbf{G}\mathbf{q} + \mathbf{h}$ and the penalty term in (3.7) can be written in the discretized form

$$(4.10)\quad \frac{1}{2}\int_C c_N\,(d\,(\mathbf{u}))^2\,dS = \frac{1}{2}\mathbf{q}^T\left\{\int_C \begin{bmatrix} -\mathbf{L}^{1T} \\ \mathbf{L}^{2T} \end{bmatrix} c_N \begin{bmatrix} -\mathbf{L}^1 & \mathbf{L}^2 \end{bmatrix} dS\,\mathbf{q} + 2\int_C \begin{bmatrix} -\mathbf{L}^{1T} \\ \mathbf{L}^{2T} \end{bmatrix} h\,dS\right\} + \text{const} = \frac{1}{2}\mathbf{q}^T \begin{bmatrix} \mathbf{C}^{11} & -\mathbf{C}^{12} \\ -\mathbf{C}^{21} & \mathbf{C}^{22} \end{bmatrix} \mathbf{q} + \mathbf{q}^T \begin{bmatrix} -\mathbf{f}_h^1 \\ \mathbf{f}_h^2 \end{bmatrix} + \text{const} = \frac{1}{2}\mathbf{q}^T\mathbf{C}\mathbf{q} + \mathbf{q}^T\mathbf{f}_h + \text{const},$$

where $\mathbf{C}$ is the contact stiffness matrix.

From the integral (3.7), the load vector $\mathbf{f}_p^e$ which corresponds to the contact pressure is

$$(4.11)\quad \int_C d\,(\mathbf{u})\,p\,dS \to \mathbf{q}^T\int_C \begin{bmatrix} -\mathbf{L}^{1T} \\ \mathbf{L}^{2T} \end{bmatrix} p\,dS = \mathbf{q}^T \begin{bmatrix} -\mathbf{f}_p^1 \\ \mathbf{f}_p^2 \end{bmatrix} = \mathbf{q}^T\mathbf{f}_p.$$

Substituting (4.7) into (2.12) we have the equilibrium equation

$$(4.12)\quad \mathbf{f}_R - \mathbf{G}_R^T\mathbf{p} = \mathbf{0},$$

where $\mathbf{f}_R$ is the external load vector and

$$(4.13)\quad \mathbf{G}_R = \int_C \begin{bmatrix} \ldots & \mathbf{n}_c\,(\mathbf{x})\,P_i\,(\mathbf{x}) & \ldots \\ \ldots & \mathbf{r}\,(\mathbf{x}) \times \mathbf{n}_c\,(\mathbf{x})\,P_i\,(\mathbf{x}) & \ldots \end{bmatrix} dS$$

is the geometrical matrix.

4.2. Discretized functionals

Finally the discretized form of the $\mathcal{L}^{LA}$ and $\mathcal{L}^{AU}$ functionals are written as:

$$(4.14)\quad \mathcal{L}^{LA} = \mathcal{L}^{LA}\,(\mathbf{q}, \mathbf{p} \geq \mathbf{0}) = \sum\nolimits_e \left\{\frac{1}{2}\mathbf{q}^{eT}\mathbf{K}^e\mathbf{q}^e - \mathbf{q}^{eT}\mathbf{f}^e\right\} + \mathbf{p}^T\,(\mathbf{G}\mathbf{q} - \mathbf{h}),$$

$$(4.15)\quad \mathcal{L}^{AU} = \mathcal{L}^{AU}\,(\mathbf{q}) = \sum\nolimits_e \left\{\frac{1}{2}\mathbf{q}^{eT}\mathbf{K}^e\mathbf{q}^e - \mathbf{q}^{eT}\mathbf{f}^e\right\} + \frac{1}{2}\mathbf{q}^T\mathbf{C}\mathbf{q} + \mathbf{q}^T\,(\mathbf{f}_h - \mathbf{f}_p).$$

By substitution of (4.7) into (3.13), the modified complementary energy has the following discretized form:

$$(4.16)\quad \mathcal{L}^C = \mathcal{L}^C\,(\mathbf{p} \geq \mathbf{0}, \lambda) = \frac{1}{2}\mathbf{p}^T\mathbf{H}\mathbf{p} + \mathbf{p}^T\mathbf{l} - \lambda^T\,(\mathbf{G}_R\mathbf{p} - \mathbf{f}_R),$$

where

$$\mathbf{H} = \frac{1}{2} \int_{S_c} \int_{S'_c} \mathbf{P}(\mathbf{x}) \left(H^1(\mathbf{x}, \mathbf{x}') + H^2(\mathbf{x}, \mathbf{x}') \right) \mathbf{P}^T(\mathbf{x}') \, dS' dS = \mathbf{H}^1 + \mathbf{H}^2$$

is the influence matrix, and

$$\mathbf{l} = \int_{S_c} \mathbf{P} \left(u^2_{N,\text{load}} - u^1_{N,\text{load}} + h \right) dS$$

is a displacement vector due to the external load and initial gap.

4.3. Systems of algebraic inequalities

Seeking the extremum of the functions (4.14), (4.16) and taking the Kuhn-Tucker conditions into consideration, the following formulae can be written

$$\frac{\partial \mathcal{L}^{LA}}{\partial \mathbf{q}^e} = \mathbf{0}, \qquad \mathbf{d} = -\frac{\partial \mathcal{L}^{LA}}{\partial \mathbf{p}} \geq \mathbf{0}, \qquad \mathbf{p} \geq \mathbf{0}, \qquad \mathbf{p}^T \mathbf{d} = 0, \tag{4.17}$$

$$\frac{\partial \mathcal{L}^{C}}{\partial \lambda} = \mathbf{0}, \qquad \mathbf{d} = \frac{\partial \mathcal{L}^{C}}{\partial \mathbf{p}} \geq \mathbf{0}, \qquad \mathbf{p} \geq \mathbf{0}, \qquad \mathbf{p}^T \mathbf{d} = 0. \tag{4.18}$$

If the determinant of matrix $\mathbf{K}^e$ is not zero, the vector $\mathbf{q}^e$ can be expressed from the following equation

$$\frac{\partial \mathcal{L}^{LA}}{\partial \mathbf{q}^e} = \mathbf{0} = \mathbf{K}^e \mathbf{q}^e + \mathbf{G}^{eT} \mathbf{p} - \mathbf{f}^e, \tag{4.19}$$

and we may substitute it into the inequality (4.17). After some straightforward transformations the compliance matrix is written as

$$\mathbf{H}^e = \mathbf{G}^e \left(\mathbf{K}^e \right)^{-1} \mathbf{G}^{eT}, \tag{4.20}$$

the displacement vector is

$$\mathbf{u}^e_{\text{load}} = -\mathbf{G}^e \left(\mathbf{K}^e \right)^{-1} \mathbf{f}^e, \tag{4.21}$$

and using (4.20) and (4.21), we have the gap in a discretized form

$$\mathbf{d} = \left(\mathbf{H}^1 + \mathbf{H}^2 \right) \mathbf{p} + \mathbf{u}^2_{\text{load}} + \mathbf{u}^1_{\text{load}} + \mathbf{h} \geq \mathbf{0}. \tag{4.22}$$

Let us consider the contact problem when the punch (body 1) has performed a rigid body translation, that is $\det \mathbf{K}^1 = 0$.

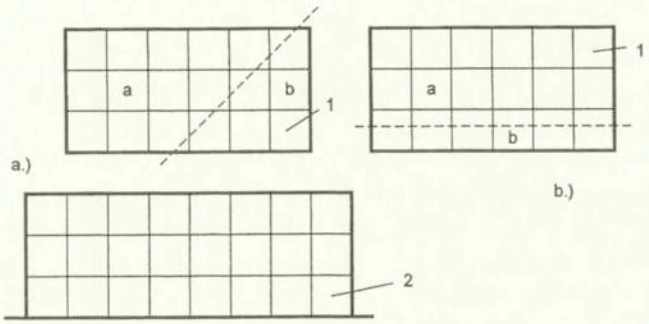

FIG. 2. Two variants for dividing the punch (body 1) into two parts denoted by a and b, (the variant b is recommended).

Let us partition (4.17) of the body 1 in such a way

$$\begin{bmatrix} \mathbf{K}_{aa} & \mathbf{K}_{ab} \\ \mathbf{K}_{ba} & \mathbf{K}_{bb} \end{bmatrix}^1 \begin{bmatrix} \mathbf{q}_a \\ \mathbf{q}_b \end{bmatrix}^1 + \begin{bmatrix} \mathbf{G}_a^T \\ \mathbf{G}_b^T \end{bmatrix}^1 \mathbf{p} = \begin{bmatrix} \mathbf{f}_a \\ \mathbf{f}_b \end{bmatrix}^1, \tag{4.23}$$

that the matrix block $\mathbf{K}_{aa}^1$ is not singular (see Fig. 2). Expressing $\mathbf{q}_a^1$ from the first equation and substituting it into the second one, we have an equation in the reduced form:

$$\mathbf{K}_{\text{red}}^1 \mathbf{q}_b^1 + \mathbf{G}_{\text{red}}^{1T} \mathbf{p} = \mathbf{f}_{\text{red}}^1, \tag{4.24}$$

where

$$\mathbf{K}_{\text{red}}^1 = \left[\mathbf{K}_{bb} - \mathbf{K}_{ba} \left(\mathbf{K}_{aa}\right)^{-1} \mathbf{K}_{ab}\right]^1,$$

$$\mathbf{G}_{\text{red}}^{1T} = \left[\mathbf{G}_b^T - \mathbf{K}_{ba} \left(\mathbf{K}_{aa}\right)^{-1} \mathbf{G}_a^T\right]^1,$$

$$\mathbf{f}_{\text{red}}^1 = \left[\mathbf{f}_b - \mathbf{K}_{ba} \left(\mathbf{K}_{aa}\right)^{-1} \mathbf{f}_a\right]^1.$$

Passing to the target (body 2), three Eqs. (4.19) – (4.21) remain valid in their original forms. Then

$$\mathbf{d} = -\frac{\partial \mathcal{L}^{LA}}{\partial \mathbf{p}} = -\mathbf{G}\mathbf{q} + \mathbf{h} = -\begin{bmatrix} \mathbf{G}_a^1 & \mathbf{G}_b^1 & \mathbf{G}^2 \end{bmatrix} \begin{bmatrix} \mathbf{q}_a^1 \\ \mathbf{q}_b^1 \\ \mathbf{q}^2 \end{bmatrix} + \mathbf{h} \tag{4.25}$$

$$= -\mathbf{G}_{\text{red}}^1 \mathbf{q}_b^1 + \left(\mathbf{H}^1 + \mathbf{H}^2\right) \mathbf{p} + \mathbf{u}_{\text{load}}^2 + \mathbf{u}_{\text{load}}^1 + \mathbf{h} \geq \mathbf{0},$$

where

$$\mathbf{H}^1 = \mathbf{G}_a^1 \left(\mathbf{K}_{aa}^1\right)^{-1} \mathbf{G}_a^{1T}, \qquad \mathbf{u}_{\text{load}}^1 = -\mathbf{G}_a^1 \left(\mathbf{K}_{aa}^1\right)^{-1} \mathbf{f}_a^1.$$

Knowing Eqs. (4.24) and (4.25), the system of inequalities to be solved has the form

$$\begin{bmatrix} \mathbf{H}^1 + \mathbf{H}^2 & -\mathbf{G}_{\text{red}}^1 \\ -\mathbf{G}_{\text{red}}^{1T} & -\mathbf{K}_{\text{red}}^1 \end{bmatrix} \begin{bmatrix} \mathbf{p} \\ \mathbf{q}_b^1 \end{bmatrix} + \begin{bmatrix} \mathbf{u}_{\text{load}}^2 + \mathbf{u}_{\text{load}}^1 + \mathbf{h} \\ \mathbf{f}_{\text{red}}^1 \end{bmatrix} = \begin{bmatrix} \mathbf{d} \\ \mathbf{0} \end{bmatrix}, \tag{4.26}$$

$$\mathbf{p} \geq \mathbf{0}, \qquad \mathbf{d} \geq \mathbf{0}, \qquad \mathbf{p}^T \mathbf{d} = 0.$$

The matrices $\mathbf{H}^e$ $(e = 1, 2)$ are constructed by the solutions of loads P_i $(i = 1, ..., KONT)$ applied to both of the bodies [19]. The rigid body displacements and rotations should be constrained and the P_i load must be equilibrated by appropriately chosen external loads.

There is another approach, when the matrices are blocked as it is shown in Fig. 2b, that is $\mathbf{G}_a^1 = \mathbf{0}$, which involves also $\mathbf{H}^1 = \mathbf{0}$ for the punch (body 1). The size of the vector $\mathbf{q}_b^1$ can be reduced to the degrees of freedom located on the contact surfaces in a similar way as it is applied in the sub-structural technique. From (4.18) we have the following inequality system which is formally similar to (4.26):

$$\begin{bmatrix} \mathbf{H}^1 + \mathbf{H}^2 & -\mathbf{G}_R \\ -\mathbf{G}_R^T & \mathbf{0} \end{bmatrix} \begin{bmatrix} \mathbf{p} \\ \lambda \end{bmatrix} + \begin{bmatrix} \mathbf{l} \\ \mathbf{f}_R \end{bmatrix} = \begin{bmatrix} \mathbf{d} \\ \mathbf{0} \end{bmatrix}, \tag{4.27}$$

$$\mathbf{p} \geq \mathbf{0}, \qquad \mathbf{d} \geq \mathbf{0}, \qquad \mathbf{p}^T \mathbf{d} = 0.$$

The algebraic system of equations associated with (4.15) can be written as follows:

$$\begin{bmatrix} \mathbf{K}^1 + \mathbf{C}^{11} & -\mathbf{C}^{12} \\ -\mathbf{C}^{21} & \mathbf{K}^2 + \mathbf{C}^{22} \end{bmatrix} \begin{bmatrix} \mathbf{q}^1 \\ \mathbf{q}^2 \end{bmatrix} = \begin{bmatrix} \mathbf{f}^1 + \mathbf{f}_h^1 - \mathbf{f}_p^1 \\ \mathbf{f}^2 - \mathbf{f}_h^2 + \mathbf{f}_p^2 \end{bmatrix} \tag{4.28}$$

where the matrix $\mathbf{C}^{ij}$ is modified to fulfill the contact/separation conditions.

The iterational KALKER procedure [11, 20] with the control of the sign of p can be applied for solving (4.26) – (4.28). The contact conditions are checked in the Gauss or Lobatto integration points of the contact elements during the solution of (4.28). Knowing the updated contact pressure $p^{(k+1)}$, the integrals (4.10) and (4.11) can be computed again, that is we have a new penalty (contact) matrix $\mathbf{C}$, and new vectors $\mathbf{f}_h$ and $\mathbf{f}_p$. The $(k+1)th$ displacements are obtained from the solution of (4.28). The procedure is terminated when the following condition is fulfilled:

$$\frac{\int\limits_{S_c} \left| p^{(k+1)} - p^{(k)} \right| dS}{\int\limits_{S_c} p^{(k+1)} dS} \leq 10^{-4}. \tag{4.29}$$

REMARKS

1. Since $d(\mathbf{u})$ is computed in a local coordinate system, the elements which have boundaries on the contact surface, must be transformed from the global coordinate system to the local one. The transformation is performed by the least squares fitting [18].

2. When the p-version is used, then accuracy is typically high enough for singularities to induce oscillations in the numerical solutions. The oscillations are minimized when nodes are located at the boundary of the contact zone. In the contact problems when the ends of contact zone are not situated in nodal points, the derivatives of the shape functions cannot have the appropriate jumps there. By moving the nodal points to the ends of the contact zone C, the jump in the derivatives can be represented in the discretized problem. The positioning technique can be found in [18].

3. The system of inequalities (4.26) and (4.27) is a Linear Complementary Problem, which can be solved by different algorithms as given e.g. in [21, 22] and [23].

4. In the work [24], a two-level algorithm is employed for solution of the contact problem using Lagrangian multipliers.

5. Contact pressure optimization problems

In optimization problems, the design parameters are usually concerned with material parameters, shape, characteristic dimensions (wall thickness, cross-sections), support system, loads, inner links, reinforcement and topology MRÓZ [25]. The sensitivity analysis is related to optimal design problems where design variables are to be determined by requiring minimization/maximization of the objective function subjected to specific design constraints. The references [5, 26, 27, 28] are using the sensitivity analysis for solution of the contact optimization problems.

The contact pressure optimization was investigated for the elastic punch and rigid target problem in case of linear elasticity. It was proved that designing the shape of a rigid body in contact with a fixed linear 2D elastic body by minimizing the potential energy under an isoparametric constraint, results in a uniform contact pressure distribution [3, 29, 30].

At some situations when the shape of an elastic body with a flat rigid foundation is chosen, the displacement gradients must be small [31].

In many earlier works [2, 7, 32], the maximum contact pressure was chosen as the objective function, but it was not differentiable. The articles [5, 29, 30] and [4] are using the total potential energy as a cost function, and the integral of the gap function as the isoparametric constraint. It is interesting that such a cost function is differentiable despite the fact that the mapping from design to state (displacement, stress) is not.

In many practical problems the bodies are in contact, therefore the elimination of the stress singularities is an important engineering task. In order to overcome this problem, application of the contact pressure control is recommended, which assures smooth contact pressure distribution as well as zero value on the border of the contact zone. We note that the constant contact pressure does not satisfy these conditions. This work extends the results of [12, 13, 14] by including rigid-body displacement and rotation of the punch.

5.1. Control of the contact pressure

In our optimization problems we suppose that the bodies are in contact on the whole sub-domain Ω_c of the contact zone $S_c = \Omega$. The contact surface is modified so that the following function is held for the contact pressure

$$p(\mathbf{x}) = v(\mathbf{x})\, p_{\max}, \qquad \mathbf{x} \in \Omega_c, \tag{5.1}$$

where the chosen control function must satisfy the condition $0 \leq v(\mathbf{x}) \leq 1$, and $p_{\max} = \max\ p(\mathbf{x})$, $\mathbf{x} = [s \quad t]$, where s and t are surface coordinates in the region Ω.

In the sub-domain Ω_{nc} ($\Omega = \Omega_c \cup \Omega_{nc}$) the satisfaction of the following inequality is required:

$$\chi(\mathbf{x}) = v(\mathbf{x})\, p_{\max} - p(\mathbf{x}) \geq \mathbf{0}, \qquad \mathbf{x} \in \Omega_{nc}. \tag{5.2}$$

Let us define a function $V(s)$ of class C^1 in the subregion Ω_c:

$$\begin{aligned}
&V(s) = 0, \quad 0 \leq s \leq L_1,\\
&V(s) = 3\left[\frac{(s-L_1)}{(L_2-L_1)}\right]^2 - 2\left[\frac{(s-L_1)}{(L_2-L_1)}\right]^3, \quad L_1 \leq s \leq L_2,\\
&V(s) = 1, \quad L_2 \leq s \leq L_3,\\
&V(s) = 1 - 3\left[\frac{(s-L_3)}{(L_4-L_3)}\right]^2 + 2\left[\frac{(s-L_3)}{(L_4-L_3)}\right]^3, \quad L_3 \leq s \leq L_4,\\
&V(s) = 0, \quad L_4 \leq s \leq L.
\end{aligned} \tag{5.3}$$

In this case $\dfrac{dV}{ds} = 0$ at $s = L_1$ and $s = L_4$ (see Fig. 3).

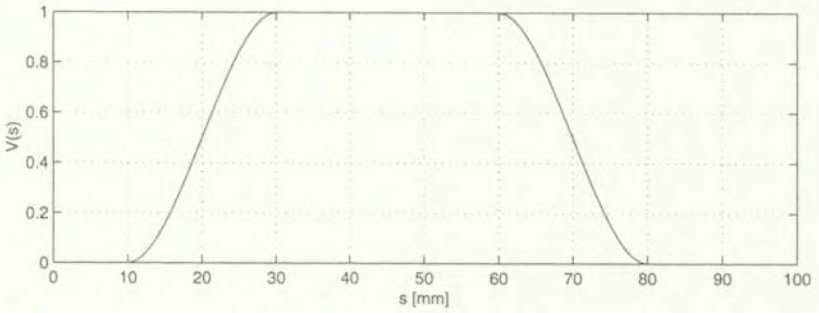

FIG. 3. Function $V(s)$ in Ω_c $L_1 = 10$, $L_2 = 30$, $L_3 = 60$, $L_4 = 80$, $L = 100$.

In 2D contact problems $v(s) = V(s)$ in Ω.

In 3D contact problems it is supposed that the punch (body 1) is subject to rigid body translation and rotation, Ω_c is a line s, and the rotation vector is perpendicular to this line. We define the controlling function along the line s in the following form:

$$v(s) = V(s)\left(1 + B\left(\frac{s}{L}\right)^n\right), \tag{5.4}$$

where B can be determined from equilibrium equations of the punch, n strongly influences the shape of $v(s)$; it is recommended to choose it from the interval $10 \leq n \leq 15$. In the direction t we introduce a simple function $\tilde{v}(t) = 1$, thus the controlling function is defined on Ω as

$$v(\mathbf{x}) = v(s)\,\tilde{v}(t). \tag{5.5}$$

5.2. Formulation of the optimization problem for axisymmetric bodies

The axially symmetric problem shown in Fig. 4 is discretized by p-extension elements. The geometry of the punch is given by inner radius $R_b = 20$ mm and outer radius $R_k = 120$ mm. There are 5 elements in radial direction ($nelr = 5$), and 3 elements in axial direction ($nelz = 3$). The order of approximation is $p = 8$ using the truncated space [15]. The following four problems have been analyzed:

P1. The displacement w_o is prescribed on the top surface of the punch. Using the controlling function with given parameters L_j $(j = 1, ..., 4)$, the shape optimization is performed on the punch, keeping its unloaded original length fixed in axial, direction. Denoting by $\triangle h$ the gap function, the optimization problem is given by variable $s = R - R_b$.

$$\min\{p_{\max} | p \geq 0, \quad d = d(p, \mathbf{u}, \triangle h) = 0, \quad \chi = v(s)\,p_{\max} - p(s) = 0, \quad \min \triangle h = 0\}. \tag{5.6}$$

P2. Applying the displacement and controlling function of problem P1, the shape optimization is performed on the punch yielding a given value of compressive force F_p

$$\min \left\{ p_{\max} | p \geq 0, \quad d = d(p, \mathbf{u}, \triangle h) = 0, \quad \chi = 0 \quad F_p = 2\pi \int_{R_b}^{R_k} Rp \, dR \right\}. \tag{5.7}$$

P3. The punch is loaded by constant pressure $\tilde{p} = 100$ MPa on its top surface. Let us determine the shape of the punch using a controlling function with parameters $L_2 - L_1 = 20$ mm, $L_3 = 80$ mm, $L_4 = 100$ mm, and maximizing the torque M_T

$$\frac{M_T}{\mu} = 2\pi \int_{R_b}^{R_k} R^2 p \, dR, \tag{5.8}$$

where μ is the friction coefficient. It is evident that the maximum of the torque is achieved when only the outer corner of the punch ($R = R_k$) is in contact, and the minimum value occurs when only the inner corner of the punch ($R = R_b$) is in contact.

Since the contact force is $F_o = \pi \left(R_k^2 - R_b^2\right) \tilde{p}$, so

$$M_T^{\max} = \mu\pi \left(R_k^2 - R_b^2\right) \tilde{p} R_k, \qquad M_T^{\min} = \mu\pi \left(R_k^2 - R_b^2\right) \tilde{p} R_b. \tag{5.9}$$

Prescribing the maximum of the contact pressure $p_{\max}$, the optimization problem is formulated as follows:

$$\max \left\{ \frac{M_T}{\mu} | \, p \geq 0, \quad d = d(p, \mathbf{u}, \triangle h) = 0, \quad F = F_o - 2\pi \int_{R_b}^{R_k} Rp \, dR = 0, \right. \tag{5.10}$$

$$\left. \chi = v(s, L_1, L_2(L_1); \; L_3, L_4 \text{ fixed}) \, p_{\max} - p(s) = 0 \right\},$$

where the parameters $\mathbf{u}, L_1, \Delta h, p$ are unknown.

P4. The relative angular velocity ω of the punch is given. The shape of the contact surface is optimized in order to minimize the frictional power loss by applying the controlling function with parameters of $L_1 = 0$, $L = 20$, $L_4 - L_3 = 20$ mm. The power loss is written as

$$D = \int_{R_b}^{R_k} R\omega\mu p 2\pi R \, dR = M_T \omega. \tag{5.11}$$

The closer is the location of the resultant of the contact pressure to radius R_b, the smaller will be the frictional power loss, thus the optimization problem is formulated as

$$\min\left\{\frac{D}{\mu\omega}\,|\; p \geq 0, \quad d = d\,(p, \mathbf{u}, \triangle h) = 0, \quad F = 0,\right. \tag{5.12}$$

$$\left.\chi = v\,(s, L_1, L_2 \text{ fixed};\; L_3\,(L_4)\,, L_4)\, p_{\max} - p\,(s) = 0\right\},$$

where the parameters $\mathbf{u}, L_4, \Delta h$ and p are unknown in the case of given $p_{\max}$.

5.2.1. Iterational algorithm for the solution of P1 - P4. The above problems are discretized when we know the location of the Lobatto integration points, where the contact conditions are checked. The discretized problems are solved with a relatively fast convergent algorithm. The discretized quantities are denoted by $\mathbf{p}^{(k)}$, $p_{\max}^{(k)}$, $\mathbf{d}^{(k)}$, $\Delta\mathbf{h}^{(k)}$, $\mathbf{u}_N^{2(k)}$, $\mathbf{u}_N^{1(k)}$ in the *k-th* iteration loop. The same control function v is used in problems P1, P2, and $p_{\max}$ is given in P3, P4.

The steps of the solution process are as follows:

1. Solution of the original contact problem : $\mathbf{p}^{(0)}$, $p_{\max}^{(0)}$, $k = 0$.
2. $k = k + 1$.
3. Computation of the new $\mathbf{p}^{(k)}$ vector from the following equation

$$\chi = \mathbf{v}\, p_{\max}^{(k-1)} - \mathbf{p}^{(k)} = \mathbf{0}.$$

REMARKS

a) In the problem P2:

$$p_{\max}^{(k-1)} = \frac{F_p}{\int\limits_{R_b}^{R_k} 2\pi R v\, dR} = \frac{F_p}{I_v}.$$

b) In problems P3, P4 the function v defined by new values of L_1 or L_4 to achieve

$$\left|p_{\max}^{(k-1)} - p_{\max}\,(\text{given})\right| \leq 0.01, \qquad p_{\max}^{(k-1)} = \frac{F_o}{I_v}.$$

4. Both the separated bodies are loaded by $p^{(k)}$. In the problem P3, P4, the punch (body 1) is supported by a vertical spring element in order to solve the system of algebraic equations.
5. Evaluation of the vector $\mathbf{m}^{(k)} = \mathbf{u}_N^{1(k)} - \mathbf{u}_N^{2(k)}$.
6. Determination of the minimum value of vector $\mathbf{m}^{(k)} \to m = \min\left(m_j^{(k)}\right)$.

7. In problems P1, P3, P4

$$\Delta \mathbf{h}^{(k)} = \mathbf{m}^{(k)} - m\mathbf{e}, \qquad \mathbf{e}^T = [\ 1 \quad 1 \quad \ldots\ ].$$

In the problem P2 : $\Delta \mathbf{h}^{(k)} = \mathbf{m}^{(k)}$.

8. Solution of (4.28) using the new shape due to $\Delta \mathbf{h}^{(k)}$.
9. Checking of the convergence condition

$$htol = 2\pi \int_{R_b}^{R_k} \left| \frac{R\left(\Delta h^{(k)} - \Delta h^{(k-1)}\right)}{\Delta h^{(k)}} \right| dR \leq 0.0001 = \vartheta.$$

If $htol > \vartheta$, then back to step 2 else stop.

5.2.2. Numerical examples. Material properties of the problem shown in Fig. 4 are Young modulus $E = 2 \cdot 10^5$ MPa, Poisson's ratio $v = 0.3$. The prescribed displacement of the punch on the boundary located at $Z = 80$ mm is $w_0 = -0.15$ mm. The initial gap function is $h = 0.00004 \cdot (R - 20)^2$. The stress distribution computed on the initial shape is shown in Fig. 4b.

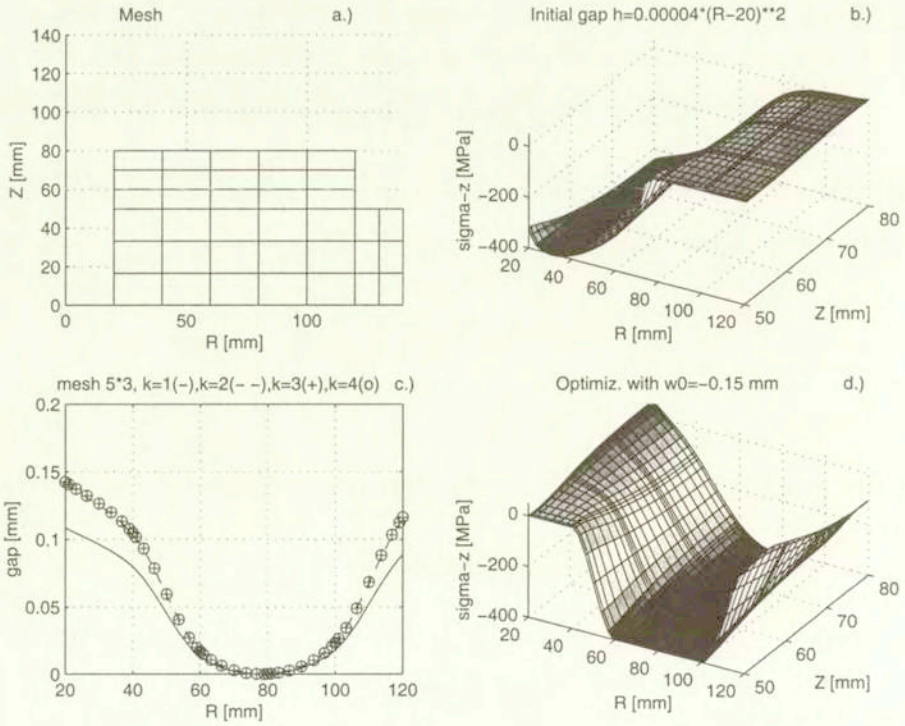

FIG. 4. The mesh of an axially symmetric problem, stress distribution σ_z in the punch, optimal solution of the initial gap and contact pressure distribution of problem P1.

Optimization problem P1. The contact optimization problem was solved by the iteration of Sec. 5.2.1, using the parameters of $L_1 = 20$ mm, $L_2 = 40$ mm, $L_3 = 80$ mm, $L_4 = 100$ mm. The modified shapes $\Delta h^{(k)}$ of the contact surface are shown in Fig. 4c for iteration loops $k = 1, 2, 3, 4$, and the final optimal normal stress is in Fig. 4d. The computed contact pressure maximum is $p_{\max} = 401.39$ MPa and torque $\dfrac{M_T}{\mu} = 6.39 \cdot 10^9$ Nmm for the optimal solution.

Optimization problem P2. The problem P2 was solved for compressive force $F_p = 5000$ kN. The shape of the contact surface is shown in Fig. 5a, the computed stresses $\sigma_R, \sigma_\varphi, \sigma_z$ are in Fig. 5b, 5c and 5d. The computed contact pressure maximum is $p_{\max} = 165.78$ MPa and torque $\dfrac{M_T}{\mu} = 2.64 \cdot 10^9$ Nmm for the optimal solution.

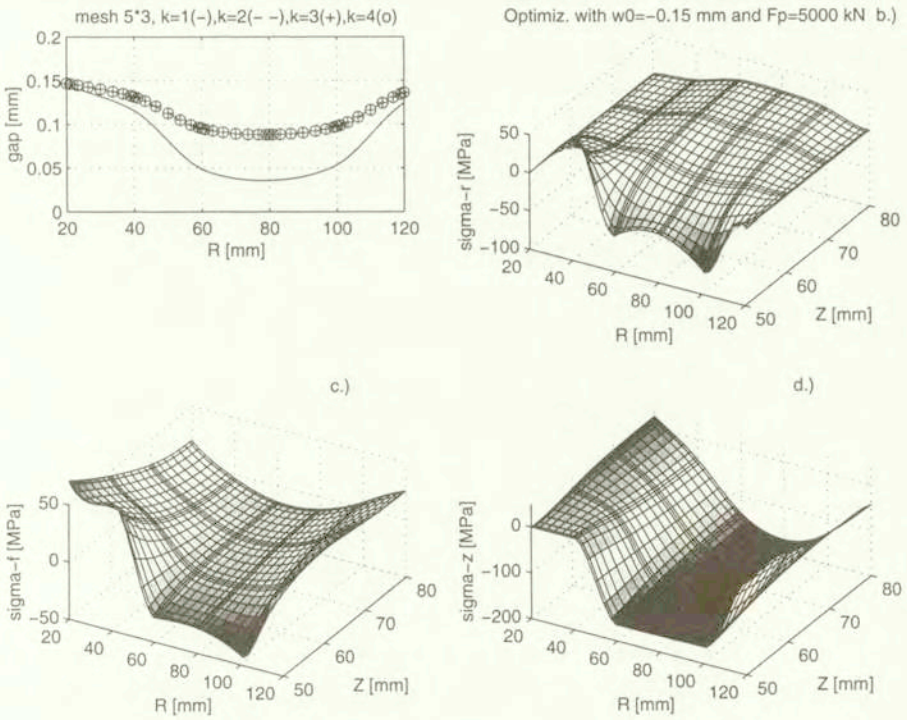

FIG. 5. Results of problem P2.

Optimization problems P3 and P4. Solving the problems P3 and P4 for given $p_{\max}$, the results of $\dfrac{M_T}{\mu}$ denoted by $(-)$ and $\dfrac{D}{\mu\omega}$ denoted by $(--)$ are shown in Fig. 6, as well as the variation of the control parameters L_1 and L_4. The above

optimizations were performed within 5 loops satisfying the tolerance in step 9 of algorithm 5.2.1.

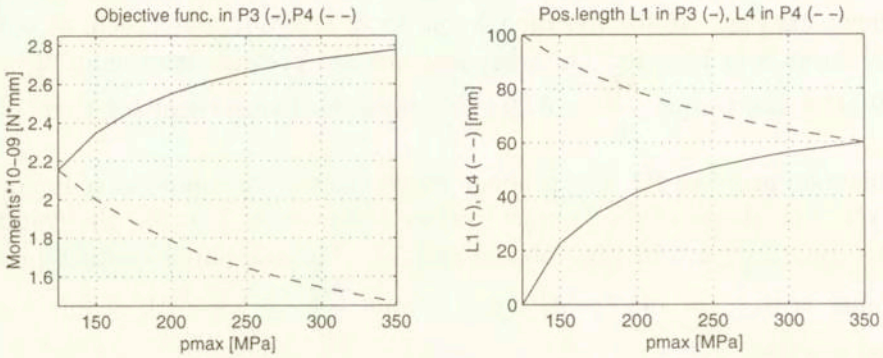

FIG. 6. The results of torque $\frac{M_T}{\mu}$, and parameters L_1, L_4 for problems P3 and P4.

5.3. Optimal shape design of the rollers

In engineering practice the roller is a frequently applied machine element. The meridian curve of the roller strongly influences the maximum of the contact pressure and its distribution, too. Due to the symmetry, a quarter of the model will be investigated, assuming linear elasticity and frictionless contact.

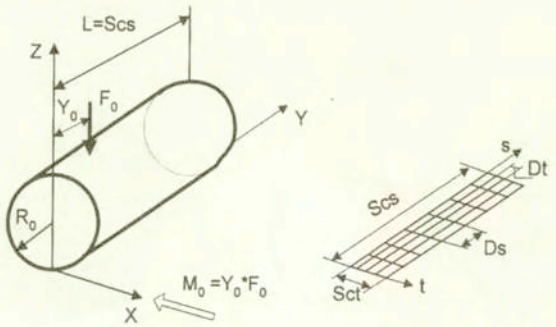

FIG. 7. Geometry and the loads of the roller, and the contact surface $\Omega = Scs \times Sct$ is divided into small elements having dimensions $Ds \times Dt$.

The loads of a roller consist of a resultant force F_o and a couple M_o; furthermore, the roller has a rigid body translation in the direction Z and rigid body rotation around X which is perpendicular to the axis of the roller (see Fig. 7). Since the contact region is sufficiently narrow in comparison to the diameter of the roller R_o, we shall apply the formulation which is valid for the elastic halfspace

to produce the influence function for the roller too, taking the mirror technique [12] into account. On the surface of the halfspace at $Z = 0$, the rectangular region $(Sct \times Scs)$ will be subdivided into small rectangles $(Dt \times Ds)$. Due to the symmetry of the contact problem with respect to the axis Y, we take only one the half of the original construction into consideration.

Elements of the influence matrix $\mathbf{H}$ are computed by applying the unit intensity normal load on six subregions $(Dt \times Ds)$ to the roller (the punch), and on four subregions to the quarter elastic space (the target, with $0 \leq Y \leq \infty$, $-\infty \leq X \leq \infty$, $-\infty \leq Z \leq 0$) in order to eliminate shearing stresses at the bottom and top surfaces of the roller and at the side $Y = 0$ of the quarter space.

Here the controlling region Ω_c is defined as a subregion of $0 \leq t \leq Dt$, $0 \leq s \leq Scs$.

Equilibrium equations for the roller are written as

$$F = F(B, p_{\max}, p \geq 0) = F_o - p_{\max} \int_{\Omega_c} v(s,t)\, dS - \int_{\Omega_{nc}} p\, dS = 0,$$

(5.13)

$$M = M(B, p_{\max}, p \geq 0) = M_o - p_{\max} \int_{\Omega_c} Y(s)\, v(s,t)\, dS - \int_{\Omega_{nc}} Yp\, dS = 0,$$

where the condition $\chi(\mathbf{x}) \geq \mathbf{0}$ must be satisfied. We obtain a formula for B using (5.3) for $V(s) = V(s, L_j)$ $\quad (j = 1, ..., 4)$:

$$B^{(i+1)} = \frac{\left(\dfrac{\displaystyle\int_{\Omega_{nc}} (Y_o - Y)\, p^{(i)} dS}{Dt \cdot p_{\max}^{(i)}} + \displaystyle\int_0^L (Y_o - Y(s))\, V(s, L_j)\, ds \right)}{- \displaystyle\int_0^L (Y_o - Y(s))\, V(s, L_j) \left(\frac{s}{L}\right)^n ds}. \tag{5.14}$$

Keeping the parameters L_j, $(j = 1, \ldots, 4)$ fixed, the pressure could be even negative in the region Ω_c $(Y_o \leq L/2)$ depending on the values of F_o and M_o. Therefore keeping the parameters L_1, L_2, $(L_4 - L_3)$ fixed, as in problem P4, the parameter L_4 is modified until the condition $v(s, 0) \geq 0$ is satisfied everywhere. It is supposed that the change of gap in region Ω_{nc} is expressed by the function of gap's change Δh in region Ω_c: $\Delta h_{nc} = f(\Delta h)$.

The optimization problem is

$$\min\{p_{\max} |\, p \geq 0, \quad d = d(p, \lambda, \Delta h) \geq 0, \quad pd = 0 \quad \mathbf{x} \in \Omega, \tag{5.15}$$

$$\chi = 0 \quad \mathbf{x} \in \Omega_c, \quad \chi \geq 0 \quad \mathbf{x} \in \Omega_{nc}, \quad F = 0, \quad M = 0\}.$$

Discretizing (5.15), in view of (4.16), (4.18), (4.27), we have a restricted linear programming problem:

$$\min\{p_{\max} |\, \mathbf{p} \geq \mathbf{0}, \quad \mathbf{d} = \mathbf{H}\mathbf{p} - \mathbf{G}_R\lambda + \mathbf{l} + \Delta\mathbf{h} \geq \mathbf{0}, \quad \mathbf{p}^T\mathbf{d} = 0, \tag{5.16}$$

$$\chi = \mathbf{v}p_{\max} - \mathbf{p} \geq \mathbf{0} \quad \mathbf{G}_R^T\mathbf{p} - \mathbf{f}_R = \mathbf{0}\}.$$

The following algorithm is proposed to solve it.

5.3.1. Iterational process of solution of the contact optimization problem (5.16).

1. Solution of the original contact problem $\left(\mathbf{p}^{(0)}, \lambda^{(0)}\right)$.
2. Determination of B from (5.14) in which $\Omega_{nc} = 0$, $i = 1$.
3. Computation of the new vector $\mathbf{p}_c$

$$\mathbf{p}^T = [\ \mathbf{p}_c^T \quad \mathbf{p}_{nc}^T\ ], \qquad \mathbf{p}_{\max}^{(0),i} = \frac{\left(p_{\max}^{(0)} + p_{\min}^{(0)}\right)^{(i-1)}}{2},$$

$$\chi_c = \mathbf{v}\left(s, B^{(0)}, L_j\right) p_{\max}^{(0),i} - \mathbf{p}_c^{(0),i} = \mathbf{0} \quad \rightarrow \quad \mathbf{p}_c^{(0),i}, \quad i = i + 1.$$

If the vector $\mathbf{p}_c^{(0),i}$ has negative terms, the parameters $L_4, L_3(L_4)$ must be modified and go to step 2 else go to step 4.

4. $k = k + 1, \qquad i = 1.$
5. If $k > 4$ then $B^{(k)}$ is determined from (5.14).
6. Computation of the new $\mathbf{p}$ vector:

$$6.1 \qquad \chi_c = \mathbf{v}\left(s, 0, B^{(k)}\right) p_{\max}^{(k-1),i} - \mathbf{p}_c^{(k),i} = \mathbf{0} \qquad \rightarrow \qquad \mathbf{p}_c^{(k),i},$$

$$6.2 \qquad \chi_{nc} = \mathbf{v}\left(s, t, B^{(k)}\right) p_{\max}^{(k-1),i} - \mathbf{p}_{nc}^{(k),i} \geq \mathbf{0} \qquad \rightarrow \qquad \mathbf{p}_{nc}^{(k),i},$$

$$6.3 \qquad p_{\max}^{(k-1),i+1} = \frac{\left(F_o - \int\limits_{\Omega_{nc}} p^{(k),i} dS\right)}{Dt \int\limits_0^L v\left(s, 0, B^{(k)}\right) ds},$$

6.4

$$\text{If} \quad \frac{\left| p_{\max}^{(k-1),i+1} - p_{\max}^{(k-1),i} \right|}{p_{\max}^{(k-1),i}} > tol = 0.0005 \quad \text{then} \quad i = i+1 \text{ go to 6.1.}$$

7. Computation of the residual vector in Ω_c

$$\mathbf{m}^{(k)} = -\left(\mathbf{H}\mathbf{p}^{(k)} - \mathbf{G}\lambda^{(k)} + \mathbf{l}\right), \qquad \lambda^{(1)} = \lambda^{(0)}.$$

8. Determination of the maximum value of $m_j^{(k)} \quad (j = 1, \ldots, k_s)$,

$$m = \max_j \left(m_j^{(k)}\right).$$

9. Determination of the change in radius of the roller

$$\Delta \mathbf{r}_{(k_s,1)}^{(k)} = \left(\mathbf{m}_c^{(k)}{}_{(k_s,1)} - m\mathbf{e}\right), \qquad \mathbf{e}^T{}_{(k_s,1)} = \left[\begin{array}{cccc} 1 & 1 & \ldots & 1 \end{array}\right].$$

10. Computation of the gap change due to the radius change

$$\Delta \mathbf{h}^{(k)} = \mathbf{Q}\Delta \mathbf{r}^{(k)},$$

where $\mathbf{Q}$ is a suitable matrix accounting for the geometry of the roller and the elements.

11. Solution of the contact problem by the new shape of the roller

$$\mathbf{d}^{(k+1)} = \mathbf{H}\mathbf{p}^{(k+1)} - \mathbf{G}_R\lambda^{(k+1)} + \mathbf{l} + \Delta \mathbf{h}^{(k)} \geq \mathbf{0}, \qquad -\mathbf{G}_R^T\mathbf{p} = -\mathbf{f}_R,$$

$$\mathbf{p}^{(k+1)} \geq \mathbf{0}, \qquad \mathbf{p}^{(k+1)T}\mathbf{d}^{(k+1)} = 0.$$

12. Checking of the convergence condition:

$$htol = \frac{\sum_{j=1}^{k_s} \left| \Delta h_j^{(k)} - \Delta h_j^{(k-1)} \right|}{\sum_{j=1}^{k_s} \left| \Delta h_j^{(k)} \right|} \leqslant 0.0025 = \vartheta.$$

If $htol \geq \vartheta$ then back to step 4, else stop and the optimization problem is solved.

5.3.2. Numerical example. The quarter of the roller and an elastic halfspace are considered. The radius of the roller is $R_o = 60$ mm. The roller is subjected to loads of $F_o = 2500$ N and $M_o = 33000$ Nmm. The proposed contact region is given by $Sct = 0.6$ mm $\times$ $Scs = 35$ mm, and it is divided into 6×60 rectangular elements, $L_1 = 0$, $L_2 = 4$ mm, $L_4 - L_3 = 4$ mm.

The contact pressure arising in case of the initial geometry is shown in Fig. 8c. The high pressure peaks are at the end of the roller ($Y = 0$).

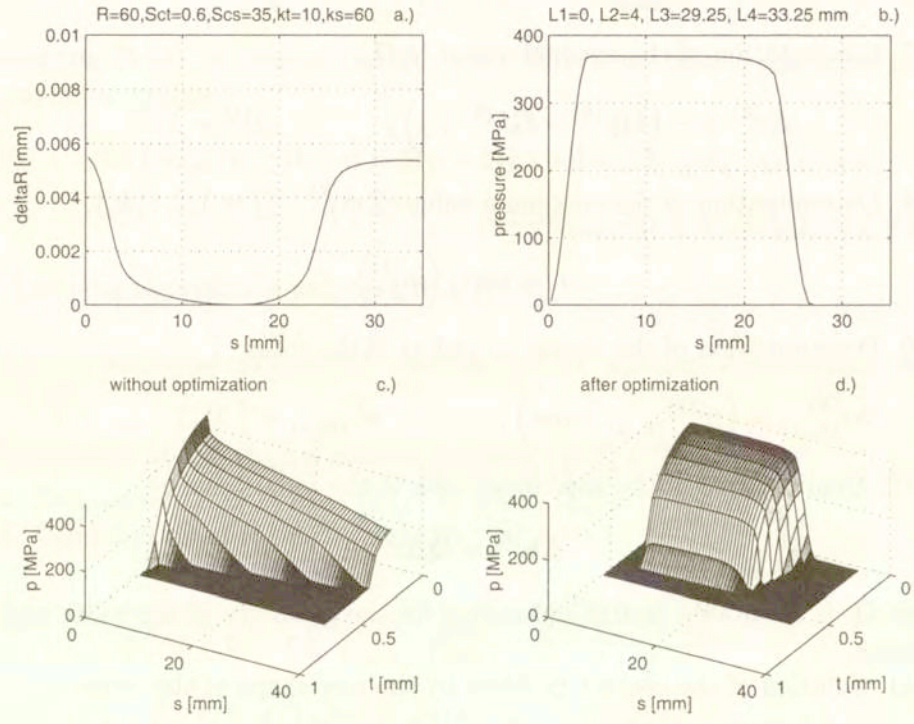

FIG. 8. Investigation of contact for the roller and the quarter space.

The optimization problem is solved for different values of n in the controlling function of $v(s,t)$. The best solution was obtained at $n = 13$, as it gave the smallest pressure value and the smoothest pressure distribution along the line $X = 0$. In case of $n > 13$, the value of the pressure maximum is larger than the value in parenthesis which is dominant around the location of $s = (L_2 + L_3)/2$. The parameters L_3 and L_4 assuring positive contact pressure and the parameter B of the controlling function are also listed in the Table 1. The *kopt* parameter denotes the number of iterations, when the tolerance of 12-*th* step of 5.3.1 is satisfied.

The computation was repeated for a higher density of mesh ($kt = 10$, $ks = 60$). The computed radius change is shown in Fig. 8a, the contact pressure distribution along the line $X = 0$ is in Fig. 8b, and the pressure distribution on the whole contact region is shown in Fig. 8d. The maximum of the contact pressure is $p_{\max}$= 369.11 MPa at $n = 13$.

Table 1.

n	$p_{\max}$ MPa	L_3 mm	L_4 mm	$B^{(0)}$	$B^{(kopt)}$	$kopt$
1	423.63	31	35	-0.9639	0.7092	23
5	372.69	24.583	28.583	−2.419	−1.5996	33
10	368.01	23.416	27.416	−11.349	−8.203	36
11	367.24	22.833	26.833	−9.516	−6.894	35
12	367.17	22.833	26.833	−14.082	−10.483	36
13	367.11	22.833	26.833	−20.734	−15.861	36
14	372.43 (366.45)	22.250	26.250	15.334	11.765	36
15	372.17 (366.47)	22.250	26.250	22.887	17.943	36
20	394.38 (366.06)	21.667	25.667	1328.29	1038.53	36

6. Conclusions

Two types of contact optimization problems have been investigated. In the first type, axially-symmetric problems are discretized by p-version finite elements. The optimizations have been performed by controlling the distribution of the contact pressure:

1. Minimizing the contact pressure maximum,
2. Minimizing the frictional power loss,
3. Maximizing the torque due to friction.

One of the advantages of using the p-version finite elements is that only coarse meshes are needed in our examples. Since high degree of polynomials ($p = 8$) is applied for the approximation of the displacement field and for mapping, the contact optimization problems have been solved with very high accuracy. Optimization problems are solved by means of a special iterative algorithm.

In the second type of the optimization problem, an optimal shape design of the rollers has been investigated. A new control function and a fast algorithm are proposed. In the optimization problem the objective function is not differentiable, the pressure is partially controlled in order to achieve smooth contact pressure. The roller may be subject to rigid body translation and rotation.

Examples are demonstrating the effectiveness of the proposed algorithms.

Acknowledgement

Financial support for this paper was provided by the grants FKFP 0040/1999, OTKA T025172 and AKP 146 2,3/31.

References

1. I. PACZELT, *Some optimization problems of contact bodies within the linear theory of elasticity*, [In:] Variational methods in the mechanics of solids, S. NEMAT-NASSER, Pergamon Press, 349–356, Oxford 1980.
2. T. F. CONRY and A. SEIREG, *A mathematical programming method for design of elastic bodies in contact*, J. Appl. Mech., **38**, 387–392, 1971.
3. A. KLARBRING, *On the problem of optimizing contact force distributions*, J. Optimiz. Theory Appl., **74**, 131–150, 1992.
4. J. PETERSON, *Behaviourally constained contact force optimization*, Structural Optimization, **9**, 189–193, 1995.
5. J. HASLINGER and P. NEITTAANMAKI, *Finite element approximation for optimal shape design*, John Wiley Sons Ltd., London 1988.
6. J. ODA, J. SAKAMOTO and K. SAN, *A method for producing a uniform contact stress distribution in composite with interface*, Structural Optimization, **3**, 23–28, 1991.
7. I. PÁCZELT and B. HERPAL, *Some remarks on the solution of contact problems of elastic shells*, Archives of Machine Structures, XXIV, 197–202, 1977.
8. K. P. OH and E. G. TRACHMANN, *A numerical procedure for designing profiled rolling*, ASME J. Lubrication Technology Series F, **98**, 68–75, 1976.
9. M. J. HARNETT, *The analysis of contact stresses in rolling element bearings*, Trans. ASME, J. Lubrication Technology Series F, **101**, 105–109, 1979.
10. Y. P. CHIU and M. J. HARNETT, *A numerical solution for the contact problem involving bodies with cylindrical surface considering cylinder effect*, ASME J. Tribology, **109**, 479–486, 1987.
11. J. M. de MUL, J. J. KALKER and B. FREDERIKSSON, *The contact between arbitrarily curved bodies of finite dimension*, ASME J. Tribology, **108**, 140–148, 1986.
12. I. PÁCZELT and T. SZABÓ, *Optimal shape design for contact problems*, Structural Optimization, **7**, 66–75, 1994.
13. I. PÁCZELT, *Some contact problems of elastic systems* [in Polish], [In:] Contact Surface Mechanics, Z. Mróz, 7–49, Polish Academy of Sciences, Warsaw 1988.
14. I. PÁCZELT, *Some new developments in contact pressure optimization*, Engng. Trans., **43**, 297–312, 1995.
15. B. A. SZABÓ and I. BABUSKA, *Finite element analysis*, John Wiley and Sons, New York 1991.
16. J. T. ODEN and N. KIKUCHI, *Contact problem in elasticity: a study of variational inequalities and finite element methods*, SIAM, Philadelphia 1988.
17. J. I. TELEGA, *Variational principles for mechanical contact problems* [in Russian], Advances of Mech., **10**, 3–95, 1987.
18. I. PÁCZELT, B. A. SZABÓ and T. SZABÓ, *Solution of contact problem using the hp-version of the finite element method*, Computers and Mathematics with Application, **38**, 4696, 1999.
19. I. PÁCZELT, *Solution of elastic contact problems by the finite displacement method*, Acta Tech. Hung., **82**, 353–375, 1976.
20. J. KALKER, *Three-dimensional elastic bodies in rolling contact*, Academic Publisher, Doordrecht 1990.

21. R. W. CATTLE, S. S. PANG and R. E. STONE, *The linear complementarity problem*, Academic Press, Boston 1992.

22. A. KLARBRING, *Mathematical programming in contact problems*, [In:] Computational Methods in Contact Mechanics, M. H. ALIABADI and C. A. BREBBIA [Eds.], Computational Mechanics Publications, pp. 233–263, Southampton 1993.

23. M. S. KUCZMA, *A viscoelastic-plastic model for skeletal structural systems with clearances*, Cames, **6**, 83–106, 1999.

24. B. NOUR-OMID and P. WRIGGERS, *A two-level iteration method for solution of contact problems*, Comput. Meths. Appl. Mech. Engng., **54**, 131–144, 1986.

25. Z. MRÓZ, *Sensitivity analysis of distributed and discretized systems*, [In:] Advanced TEMPUS Course on Numerical Methods in Computer-Aided Optimal Design, T. Burczyński, pp. 1–60, Silesian Technical University of Gliwice 1992.

26. E. A. FANCELLO and R. A. FEIJÓO, *Shape optimization in frictionless contact problems*, Int. J. Numer. Meth. Engng., **37**, 2311–2335, 1994.

27. E. FANCELLO, J. HASLINGER and R. A. FEIJÓO, *Numerical comparison between two cost functionals in contact shape optimization*, Structural Optimization, **9**, 57–68, 1995.

28. G. SZEFFER, *Shape sensitivity in contact problems of elastic bodies*, [In:] WCSMO-1, N. OLHOFF, G. I. N. ROZVANY, pp. 335–340, Pergamon Press, 1995.

29. R. l. BENEDICT and J. E. TAYLOR, *Optimal design for elastic bodies in contact*, [In:] Optimization of distributed parameter structures, Part II, E. J. HAUG, J. CEA, pp. 1553–1599, Sijthoff and Alphen aan den Rijn 1981.

30. N. KIKUCHI and J. E. TAYLOR, *Shape optimization for unilateral elastic contact problems*, [In:] Num. Meth. Coupl. Probl. University College Swansea, pp. 430–441, Wales 1981.

31. A. KLARBRING and J. HASLINGER, *On almost constant stress distributions by shape optimization*, Structural Optimization, **5**, 213–216, 1993.

32. E. J. HAUG and B. M. KWAK, *Contact stress minimization by contour design*, Int. J. Numer. Meth. Engng., **12**, 917–939, 1978.

Received February 7, 2000; revised version June 27, 2000.